

Thick Junction Photodiodes Based on Crushed Perovskite Crystal/Polymer Composite Films

Jiali Peng^{†,‡}, Lihao Cui[†], Ruiming Li[†], Yalun Xu[†], Li Jiang[†], Yuwei Li[†], Wei Li[†],
Xiaoyu Tian[†] and Qianqian Lin^{*,†}

[†] *Key Lab of Artificial Micro- and Nano-Structures of Ministry of Education of China, School of Physics and Technology, Wuhan University, Wuhan 430072, P. R. China*

[‡] *Hubei Collaborative Innovation Center for Advanced Organic Chemical Materials Ministry of Education, Key Laboratory for the Green Preparation and Application of Functional Materials, Faculty of Materials Science and Engineering, Hubei University, Wuhan, China*

Corresponding Author:

*Email: q.lin@whu.edu.cn

1. Experimental details
2. Supporting figures

1. Experimental details

Materials: Lead iodide (PbI_2 , 99% trace metals basis) was purchased from Sigma-Aldrich. Methylammonium iodide ($\text{CH}_3\text{NH}_3\text{I}$, 99.99%) was purchased from Greatcell Solar. Nickel acetate ($\text{C}_4\text{H}_{14}\text{NiO}_8$, AR, 99%) was purchased from Heowns. Polymethylmethacrylate (PMMA) were purchased from Sinopharm Chemical Reagent Co., Ltd. Fullerene-C70 (C70, >99%) and bathocuproine (BCP, >99%) were purchased from Xi'an Polymer Light Technology Corp. Gamma-Butyrolactone (GBL, >99.0%) was purchased from Tokyo Chemical Industry (TCI). Ethylene glycol monomethyl ether ($\text{C}_3\text{H}_8\text{O}_2$, AR, $\geq 99.0\%$) was purchased from Greagent. Chlorobenzene ($\text{C}_6\text{H}_5\text{Cl}$, AR, 99%) was purchased from Aladdin. Acetone ($\text{C}_3\text{H}_6\text{O}$, AR) and ethanol ($\text{C}_2\text{H}_6\text{O}$, AR, anhydrous, $\geq 99.7\%$) were purchased from Sinopharm Chemical Reagent Co., Ltd. 2-aminoethanol ($\text{C}_2\text{H}_7\text{NO}$, AR, 99%) was purchased from Aladdin. All commercial products were used as received.

Preparation of perovskite single crystal powders: The $\text{CH}_3\text{NH}_3\text{PbI}_3$ perovskite single crystals were prepared via inverse temperature crystallization^[S1]. Typically, 461 mg PbI_2 and 159 mg $\text{CH}_3\text{NH}_3\text{I}$ were added into 0.8 ml GBL solvent with a molar ratio of 1:1 to form 1.25 M perovskite precursor solution. The mixed solution was stirred and heated on a hot plate at 60°C for 2 h, and filtered (0.22 μm pore size) after all solids were dissolved. The obtained solution was transferred to clean containers, which were kept on a stable hot-plate and gradually heated to 120°C and kept for another 6 h. Crystals were formed in the bottom of the containers. Finally, the crystals were collected and dried at 60°C in vacuum oven for 12 h. Then, the single crystals were ground and sieved carefully in glovebox ($\text{O}_2 < 1$ ppm, $\text{H}_2\text{O} < 1$ ppm) to prevent materials degradation during the process, as the perovskite are sensitive to moisture. $\text{CH}_3\text{NH}_3\text{PbI}_3$ single crystal powders were collected with a vial and stored in a glovebox.

Device fabrication: All the photodetector devices were fabricated based on commercial patterned Indium Tin Oxide (ITO) substrates (Meijingyuan Glass). These electrodes were cleaned with detergent solution at 80°C , followed with sonication in sequence in de-ionized water, acetone and ethanol for 10 min each. These substrates

were dried on a hot plate at 120°C for 10 min before depositing thin films according to the device structure. The cleaned substrates were dried with nitrogen before being sustained ozone treatment for 15 min. The NiO_x precursor solution was prepared by adding 35.36 mg nickel acetate and 12.22 μL 2-aminoethanol in 1 mL ethylene glycol monomethyl ether and stirred for 1h under 70°C, according to the method reported by W. Chen *et al.*^[S2] The obtained NiO_x precursor was spin-coated on the substrates at 3000 rpm for 30 s in air to form hole transport layer (HTL). The NiO_x-coated substrates were pre-annealed at 150°C for 5 min on a hot plate, followed with another annealing treatment in a muffle furnace at 300°C for 60 min. After cooling, the substrates were transferred to a nitrogen-filled glovebox for device fabrication (O₂ < 1 ppm, H₂O < 1 ppm). 25 mg PMMA were dissolved in 0.5 mL chlorobenzene to form a viscous solution (50 mg/ml). Then, another 500 mg CH₃NH₃PbI₃ single crystal powders were added in the prepared 0.5 mL PMMA solution, followed with ultrasonication and stirring until powders were uniformly dispersed. Then, the CH₃NH₃PbI₃/PMMA suspension was spin-coated on the NiO_x layer at 500 rpm for 100 s to form thick perovskite/polymer composite films, which were annealed at 100°C for 30 min in glovebox afterwards. In order to deposit electron transfer layer, 60 nm C70 were evaporated under vacuum ($\sim 4 \times 10^{-4}$ Pa, at a rate of ~ 0.1 Å/s). Another 3 nm BCP were evaporated at the same conditions. Finally, 60 nm Cu electrodes were evaporated under vacuum ($\sim 4 \times 10^{-4}$ Pa, at a rate between 0.1 and 0.5 Å/s).

Characterization: Scanning electron microscopy (SEM) images of the films were obtained using a SIGMA 500 field-emission scanning electron microscope operated at 5 keV. The surface morphology of the perovskite films were imaged using a micro microscope. The crystal structure was characterized with X-ray diffraction (XRD) using an D8 Advance X-ray diffractometer (CuK α =1.5418 Å) with a scanning range from 10° to 80°. Film thicknesses were determined using a film thickness gauge (ThetaMetrisis, FR-Basic-UV/NIR-HR). The roughness and thickness of the crushed CH₃NH₃PbI₃ crystal/PMMA composite films were recorded with an Alpha-step D-600 profile meter (KLA-Tencor).

Device performance measurements: *J-V* characteristics (both in dark and under illumination) of the devices were tested at room temperature by using a Keithley 2400 source meter. A Xenon lamp (Solar-500) was used as light source to provide various light intensities for measuring light *J-V* curves. Frequency response were obtained using different color LEDs (Thorlabs) modulated with an arbitrary wave function generator (Agilent, 33612A), and the photocurrent responses of these devices were recorded with a digital storage oscilloscope (LeCroy Waverunner 8254). Responsivity was measured with a lock-in amplifier, and the light intensity was calibrated with a standard certified photodiode (Thorlabs).

2. Supporting figures

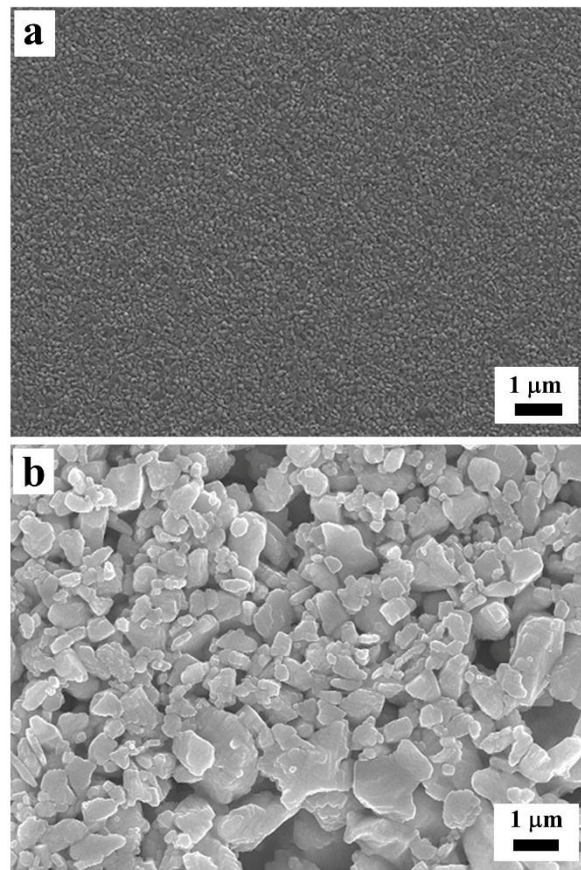


Fig. S1 SEM images of solution-processed (a) CH₃NH₃PbI₃ thin films and (b) crushed CH₃NH₃PbI₃ crystal/PMMA composite films.

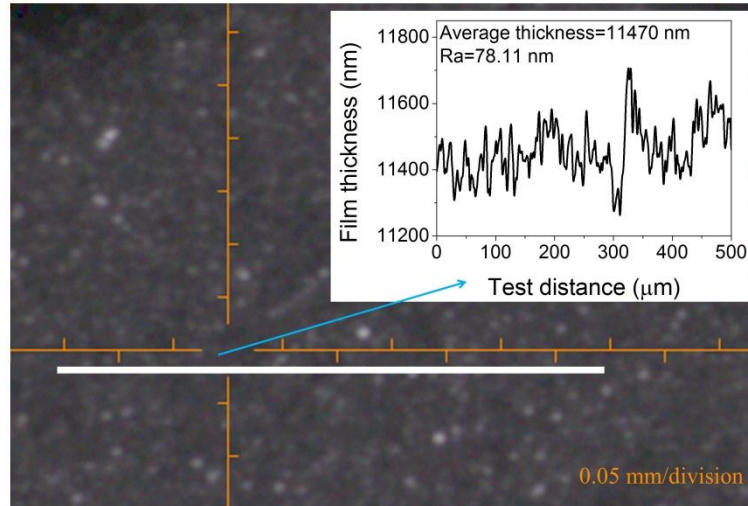


Fig. S2 Recorded roughness and thickness of the crushed $\text{CH}_3\text{NH}_3\text{PbI}_3$ crystal/PMMA composite films via profile meter.

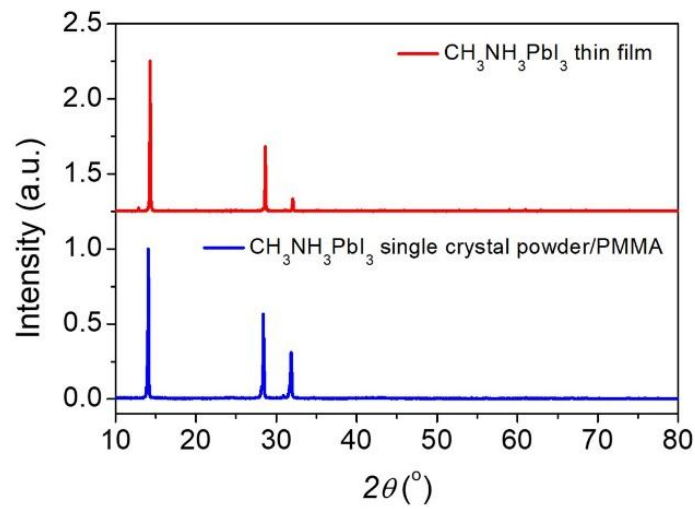


Fig. S3 Comparison of the X-ray diffraction patterns of (a) $\text{CH}_3\text{NH}_3\text{PbI}_3$ thin films and (b) crushed $\text{CH}_3\text{NH}_3\text{PbI}_3$ crystal/PMMA composite films.

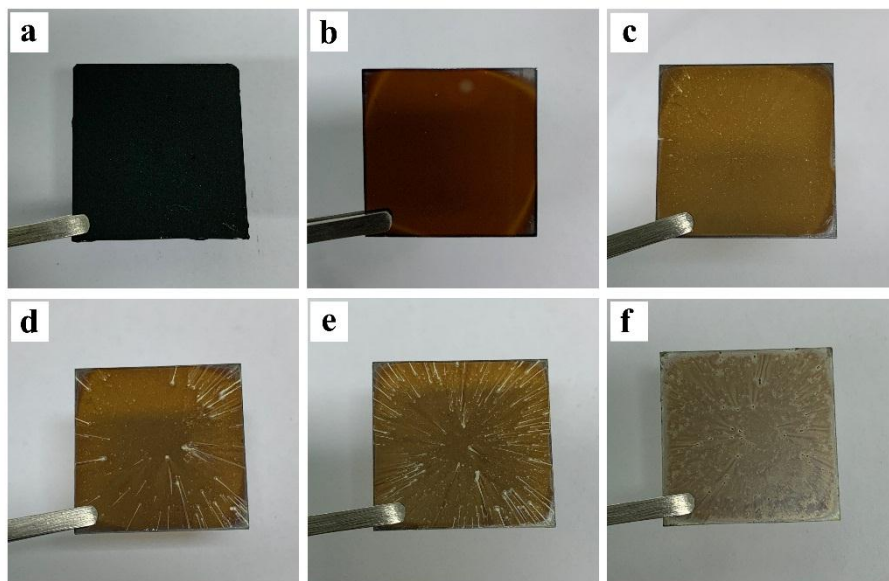


Fig. S4 Typical optical photos of (a) the crushed single crystal/PMMA composite thick films, (b) the spin-coated $\text{CH}_3\text{NH}_3\text{PbI}_3$ thin films and (c)-(f) $\text{CH}_3\text{NH}_3\text{PbI}_3$ /PMMA thin films prepared by directly mixing of PMMA and perovskite precursors with PMMA concentration of (c) 0.5 mg/mL, (d) 5 mg/mL, (e) 25 mg/mL and (f) 50 mg/mL.

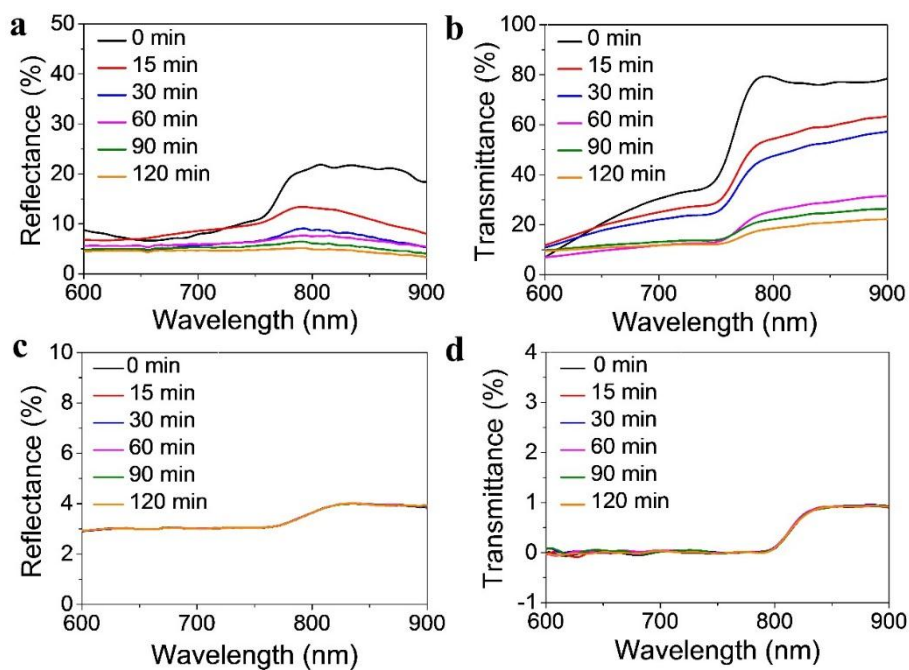


Fig. S5 Comparison of reflectance and transmittance spectra of (a), (b) $\text{CH}_3\text{NH}_3\text{PbI}_3$ thin films and (c), (d) crushed $\text{CH}_3\text{NH}_3\text{PbI}_3$ crystal/PMMA composite films.

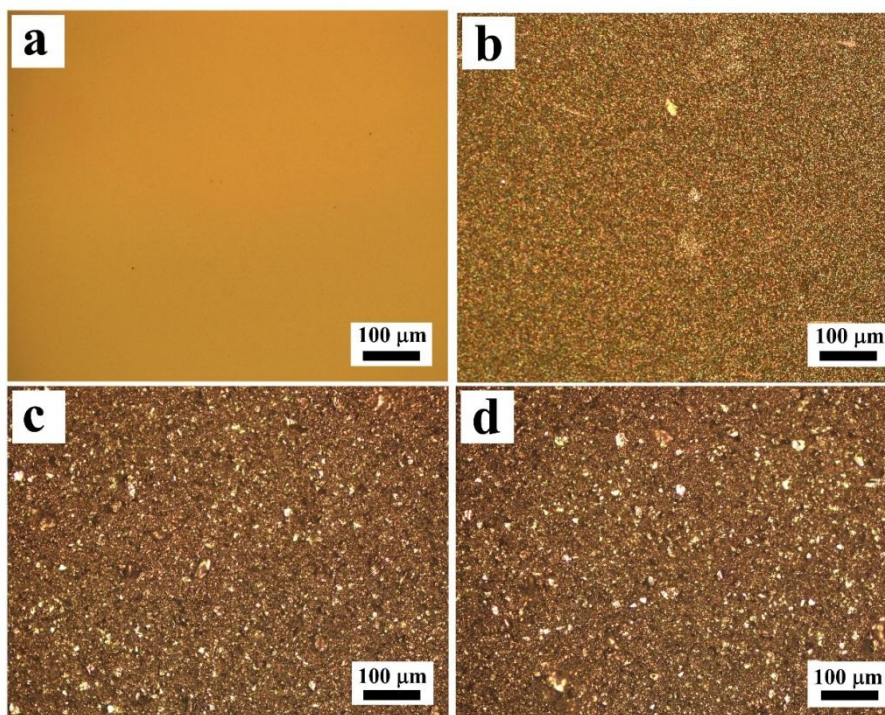


Fig. S6 Optical photos of (a) as-prepared $\text{CH}_3\text{NH}_3\text{PbI}_3$ thin films, (b) $\text{CH}_3\text{NH}_3\text{PbI}_3$ thin films exposed in air for 120 min, (c) as-prepared crushed $\text{CH}_3\text{NH}_3\text{PbI}_3$ crystal/PMMA composite films and (d) crushed $\text{CH}_3\text{NH}_3\text{PbI}_3$ crystal/PMMA composite films exposed in air for 120 min.

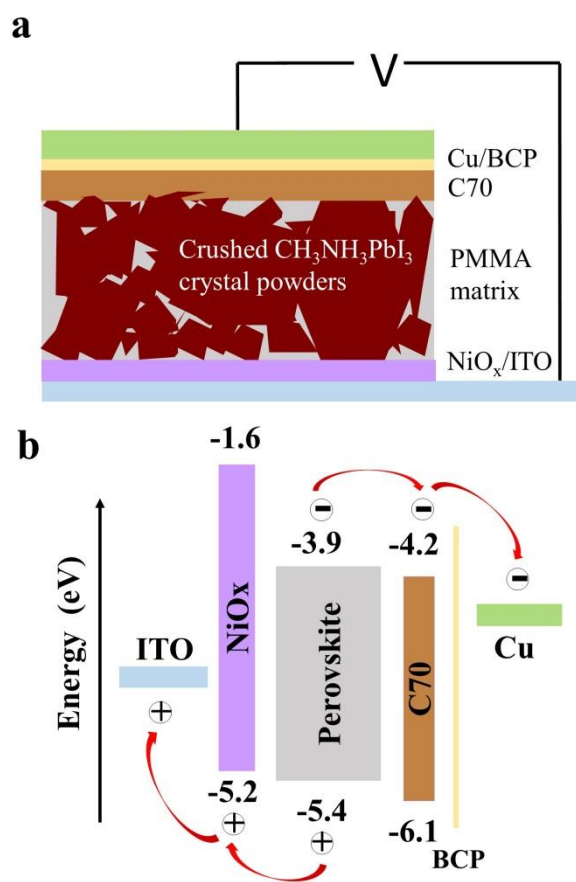


Fig. S7 Schematic illustration of (a) the device architecture of thick junction perovskite photodetectors and (b) proposed energy level diagram.

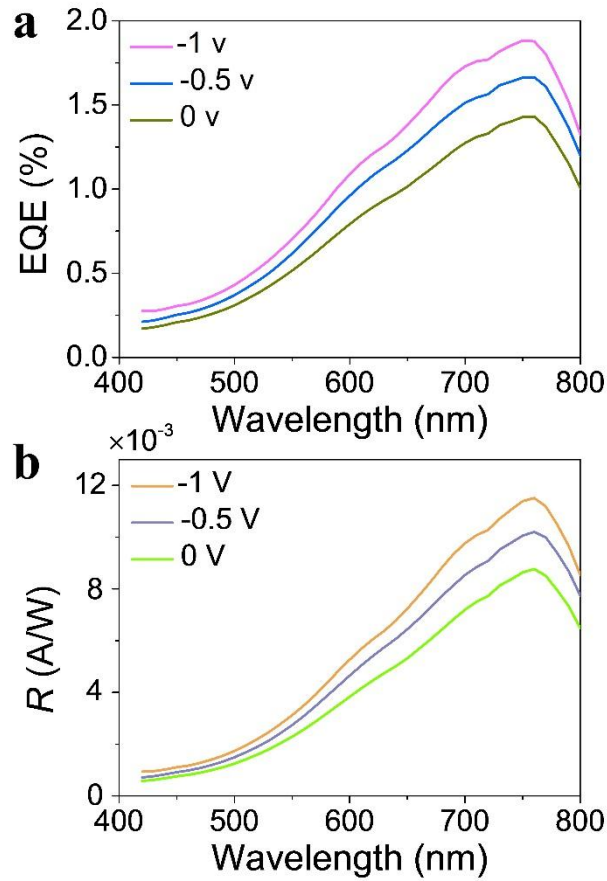


Fig. S8 (a) External quantum efficiency and (b) responsivity of the crushed $\text{CH}_3\text{NH}_3\text{PbI}_3$ crystal/PMMA composite film based TJPPDs.

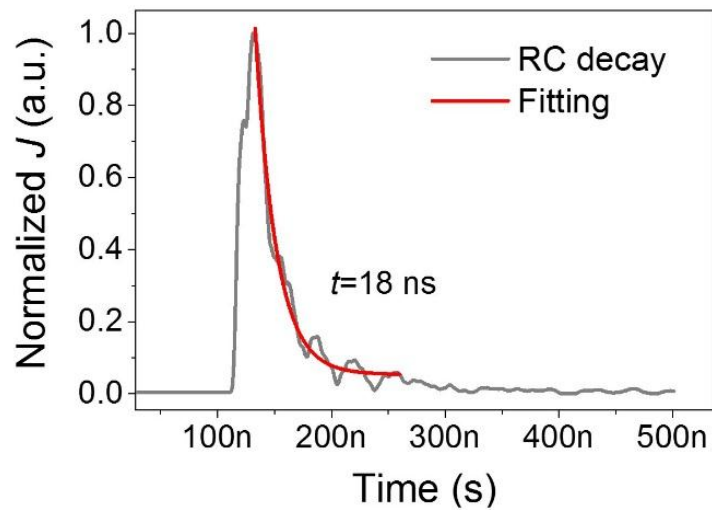


Fig. S9 Typical RC decay of the optimized thick junction photodiodes based on crushed $\text{CH}_3\text{NH}_3\text{PbI}_3$ crystal/PMMA composite films, measured with $R_{\text{load}}=100 \Omega$.

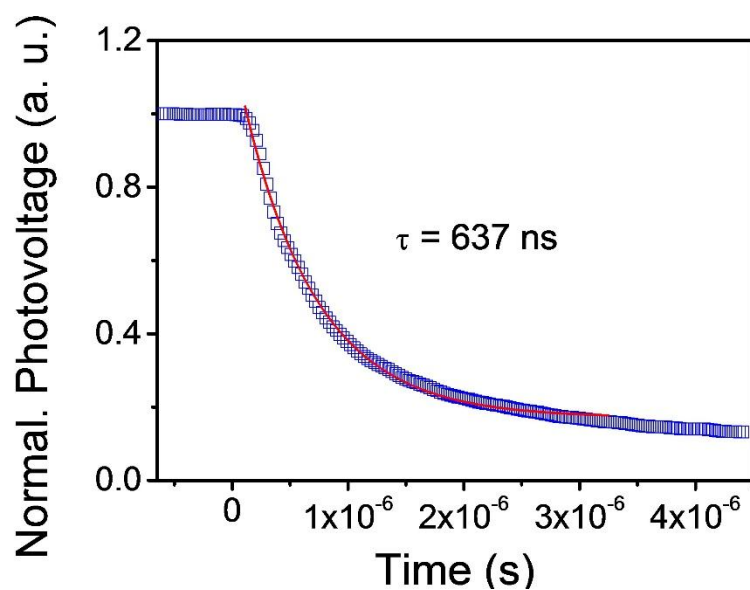


Fig. S10 Recorded photovoltage decay of the crushed $\text{CH}_3\text{NH}_3\text{PbI}_3$ crystal/PMMA composite film based TJPPDs.

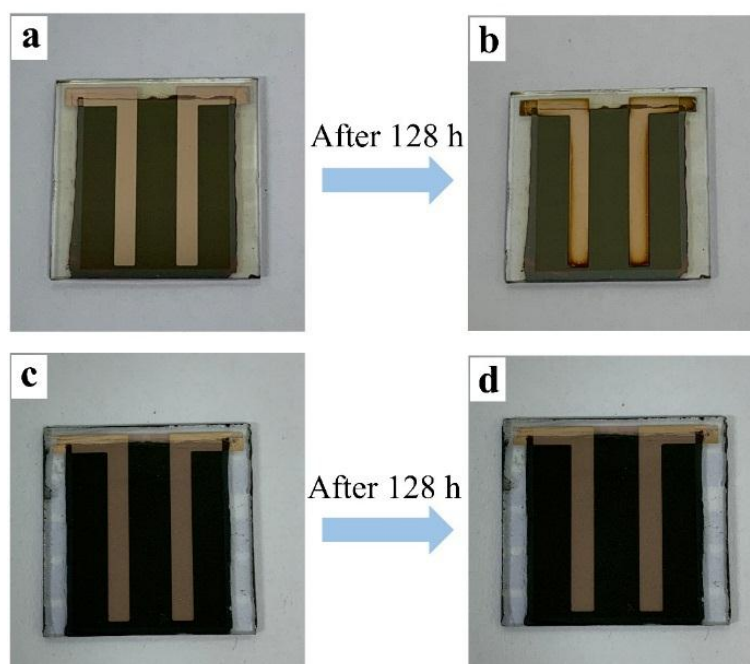


Fig. S11 Optical photos of (a) as-prepared $\text{CH}_3\text{NH}_3\text{PbI}_3$ thin film based devices, (b) $\text{CH}_3\text{NH}_3\text{PbI}_3$ thin film based devices stored in air after 128 h (20 °C/35% RH), (c) as-prepared crushed $\text{CH}_3\text{NH}_3\text{PbI}_3$ crystal/PMMA composite film based TJPPDs and (d) crushed $\text{CH}_3\text{NH}_3\text{PbI}_3$ crystal/PMMA composite film based TJPPDs stored in air after 128 h (20 °C/35% RH).

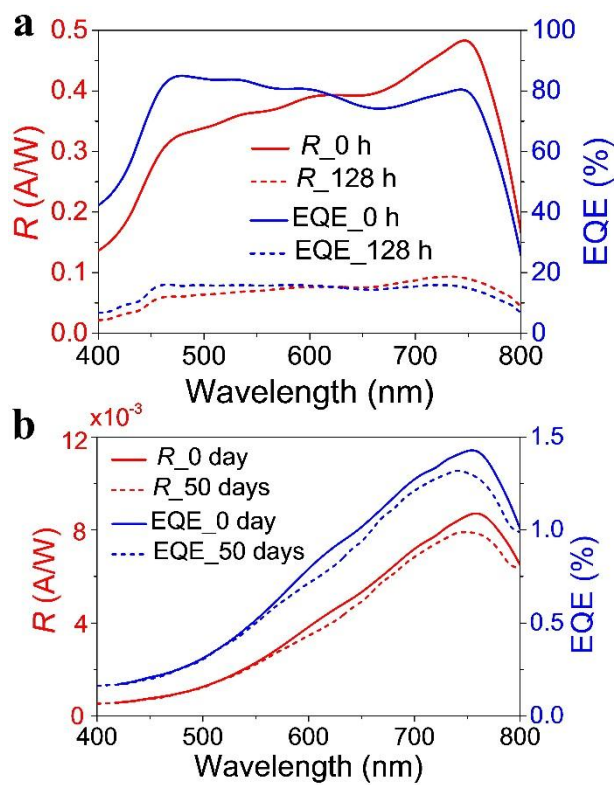


Fig. S12 Long-term stability of the responsivity and external quantum efficiency of (a) $\text{CH}_3\text{NH}_3\text{PbI}_3$ thin film based photodiodes and (b) crushed $\text{CH}_3\text{NH}_3\text{PbI}_3$ crystal/PMMA composite film based TJPPDs measured without bias.

Table S1 Comparison of the key parameters for perovskite-based photodetectors.

Active layer/charge transport length	Type	I_{noise} (A/H $Z^{1/2}$)	I_{dark} (mA/cm ²)	Response time/Frequency response	Detectivity /EQE/R	Stability	Reference
MAPbI ₃ polycrystalline film, ~300 nm	Photodiode	N/A	10 ⁻⁵ @ -1 V	N/A	4.8×10 ¹² Jones	Preserve 70% J_{ph} after exposure in air for 50 hours	Ref. S3
MAPbI ₃ polycrystalline film, 360~410 nm	Photodiode	10 ⁻¹¹	10 ⁻³ @ -1 V	~10 μs	242 A/W	N/A	Ref. S4
MAPbI _{3-x} Cl _x polycrystalline film, 200~600 nm	Photodiode	10 ⁻¹²	10 ⁻⁷ @ -1 V	~600 ns	10 ¹⁴ Jones	N/A	Ref. S5
CH ₃ NH ₃ PbI ₃ single crystal, 30 μm	Photoresistor	N/A	N/A	71 μs	0.24 A/W	N/A	Ref. S6
CH ₃ NH ₃ PbI ₃ single crystal, 60 μm	Photoresistor	N/A	10 ⁻⁶ @ 0 V	~0.2 S	7.92 A/W	N/A	Ref. S7
Crushed CH ₃ NH ₃ PbI ₃ single crystal/PMMA composites, 11.5 μm	Photodiode	3×10 ⁻¹³	10 ⁻⁵ @ -1 V	800 ns	10 ¹¹ Jones	Negligible degradation after 50 days, without encapsulation	Our work

References:

- [S1] M. I. Saidaminov, A. L. Abdelhady, B. Murali, E. Alarousu, V. M. Burlakov, W. Peng, I. Dursun, L. Wang, Y. He, G. Maculan, A. Goriely, T. Wu, O. F. Mohammed and O. M. Bakr, *Nat. Comm.*, 2015, **6**, 7586.
- [S2] W. Chen, F. Z. Liu, X. Y. Feng, A. B. Djurišić, W. K. Chan and Z. B. He, *Adv. Energy Mater.*, 2017, **7**, 1700722.
- [S3] C. Liu, K. Wang, C. Yi, X. Shi, P. Du, A. W. Smith, A. Karim and X. Gong, *J. Mater. Chem. C.*, 2015, **3**, 6600-6606.
- [S4] R. Dong, Y. Fang, J. Chae, J. Dai, Z. Xiao, Q. Dong, Y. Yuan, A. Centrone, X. C. Zeng and J. Huang, *Adv. Mater.*, 2015, **27**, 1912-1918.
- [S5] L. Dou, Y. M. Yang, J. You, Z. Hong, W. H. Chang, G. Li and Y. Yang, *Nat. Comm.*, 2014, **5**, 5404.
- [S6] J. Ding, H. Fang, Z. Lian, J. Li, Q. Lv, L. Wang, J. L. Sun and Q. Yan, *Cryst. Eng. Comm.*, 2016, **18**, 4405-4411.
- [S7] H. Fang, Q. Li, J. Ding, N. Li, H. Tian, L. Zhang, T. Ren, J. Dai, L. Wang and Q. Yan, *J. Mater. Chem. C.*, 2016, **4**, 630-636.